ARTICLE

Mutations in the N-terminal Actin-Binding Domain of Filamin C Cause a Distal Myopathy

Rachael M. Duff,[1,2] Valerie Tay,[3] Peter Hackman,[4] Gianina Ravenscroft,[1] Catriona McLean,[5] Paul Kennedy,[5] Alina Steinbach,[6] Wiebke Schöffler,[6] Peter F.M. van der Ven,[6] Dieter O. Fürst,[6] Jaeguen Song,[7] Kristina Djinović-Carugo,[7,13] Sini Penttilä,[8] Olayinka Raheem,[8] Katrina Reardon,[3] Alessandro Malandrini,[9] Simona Gambelli,[9] Marcello Villanova,[10] Kristen J. Nowak,[1] David R. Williams,[11] John E. Landers,[12] Robert H. Brown, Jr.,[12] Bjarne Udd,[4,8,14] and Nigel G. Laing[1,*]

Linkage analysis of the dominant distal myopathy we previously identified in a large Australian family demonstrated one significant linkage region located on chromosome 7 and encompassing 18.6 Mbp and 151 genes. The strongest candidate gene was *FLNC* because filamin C, the encoded protein, is muscle-specific and associated with myofibrillar myopathy. Sequencing of *FLNC* cDNA identified a c.752T>C (p.Met251Thr) mutation in the N-terminal actin-binding domain (ABD); this mutation segregated with the disease and was absent in 200 controls. We identified an Italian family with the same phenotype and found a c.577G>A (p.Ala193Thr) filamin C ABD mutation that segregated with the disease. Filamin C ABD mutations have not been described, although filamin A and filamin B ABD mutations cause multiple musculoskeletal disorders. The distal myopathy phenotype and muscle pathology in the two families differ from myofibrillar myopathies caused by filamin C rod and dimerization domain mutations because of the distinct involvement of hand muscles and lack of pathological protein aggregation. Thus, like the position of *FLNA* and *B* mutations, the position of the *FLNC* mutation determines disease phenotype. The two filamin C ABD mutations increase actin-binding affinity in a manner similar to filamin A and filamin B ABD mutations. Cell-culture expression of the c.752T>C (p.Met251)Thr mutant filamin C ABD demonstrated reduced nuclear localization as did mutant filamin A and filamin B ABDs. Expression of both filamin C ABD mutants as full-length proteins induced increased aggregation of filamin. We conclude filamin C ABD mutations cause a recognizable distal myopathy, most likely through increased actin affinity, similar to the pathological mechanism of filamin A and filamin B ABD mutations.

Introduction

The distal myopathies are a group of genetic muscle-wasting disorders characterized by muscle weakness predominantly originating in distal muscle groups of the upper or lower limbs.[1,2] Currently, the many types of distal myopathy are differentiated by the phenotypic variations within the disease spectrum. These include age at onset, affected muscle groups, severity, presence of cardiomyopathy, and mode of inheritance. The distal myopathies show either dominant or recessive inheritance, and the genetic basis for several of the distal myopathies has been determined. The known proteins affected in distal myopathies encompass a range of different types but include a significant number of sarcomeric proteins[1] (Table 1).[3–12] In addition, patients with diseases described by other terms, such as myofibrillar myopathy, also often have a distal myopathy phenotype.[2] The genetic basis of other distal myopathies, including Welander distal myopathy (WDM [MIM 604454]), one of the first distal myopathies described,[13] remains unknown.[2]

In 2005 we described in a large family from Victoria, Australia,[14] a distal myopathy sometimes termed Distal ABD-filaminopathy or William's myopathy[15]. The distal myopathy in the family did not link to any of the then known distal myopathy loci, which reinforced the novel clinical phenotype.[14] Here we have reanalyzed the clinical phenotype, reclassified the members in the family, and performed a whole-genome linkage analysis. Significant linkage for the disease in the family (multipoint LOD score 3.3) was obtained on chromosome 7. We subsequently identified a second family from Italy with the same phenotype and showed that the disease in this second family was compatible with linkage to the same region of chromosome 7. We found two different missense mutations in the N-terminal ABD of *FLNC* (MIM 102565), and both mutations segregate with the disease in the two families. Actin-binding studies of the two mutant filamin C ABDs

[1]Centre for Medical Research, University of Western Australia and Western Australian Institute for Medical Research, Perth, Western Australia 6009, Australia; [2]Centre for Neuromuscular and Neurological Disorders, University of Western Australia, Perth, Western Australia 6009, Australia; [3]Centre for Clinical Neurosciences and Neurological Research, St. Vincent's Hospital, Melbourne, Victoria 3065, Australia; [4]Folkhälsan Institute of Genetics, Department of Medical Genetics, Haartman Institute, University of Helsinki, 00014 Helsinki, Finland; [5]State Neuropathology Service, Department of Pathology, University of Melbourne, Melbourne, Victoria 3010, Australia; [6]Institute for Cell Biology, Department of Molecular Cell Biology, University of Bonn, 53121 Bonn, Germany; [7]Department for Structural and Computational Biology, Max F. Perutz Laboratories, University of Vienna, 1030 Vienna, Austria; [8]Neuromuscular Research Unit, University of Tampere, Department of Neurology Tampere University Hospital, 33520 Tampere, Finland; [9]Department Neurological, Neurosurgical and Behavioural Sciences, Unit of Neurometabolic Diseases, University of Siena, 53100 Siena, Italy; [10]Casa di Cura Nigrisoli, 40125 Bologna, Italy; [11]Van Cleef Roet Centre for Nervous Disease, Monash University, Melbourne, Victoria 3800, Australia; [12]Department of Neurology, University of Massachusetts Medical School, Worcester, MA 01605, USA; [13]Department of Biochemistry, Faculty of Chemistry and Chemical Technology, University of Ljubljana, Ljubljana 1000, Slovenia; [14]Department of Neurology, Vasa Central Hospital, 65130 Vasa, Finland
*Correspondence: nlaing@cyllene.uwa.edu.au
DOI 10.1016/j.ajhg.2011.04.021.

Table 1. Distal Myopathies with Known Genes

Disease	Gene	Protein Type
Dominant		
Tibial muscular dystrophy (TMD, Udd myopathy [MIM 600334])	Titin (*TTN* [MIM 188840])[3]	sarcomeric
Laing myopathy (MPD1 [MIM 160500])	slow skeletal/b-cardiac myosin (*MYH7* [MIM 160760])[4]	sarcomeric
Desminopathy (MIM 601419)	desmin (*DES* [MIM 608810])[1]	sarcomeric
Markesbery-Griggs distal myopathy	ZASP (*LDB3* [MIM 605906])[5]	sarcomeric
Distal myopathy with vocal cord and pharyngeal weakness (MPD2 [MIM 606070])	matrin 3 (*MATR3* [MIM 164015])[6]	nuclear matrix
Early-onset distal myopathy	kelch-like homolog 9 (*KLHL9* [MIM 611201])[58]	ubiquitylation
Recessive		
Miyoshi distal myopathy (MMD1 [MIM 254130])	dysferlin (*DYSF* [MIM 603009])[7,8]	sarcolemmal
Nonaka distal myopathy (NM [MIM 605820])/ hereditary inclusion body myopathy (IBM2 [MIM 600737])	UDP-N-acetylglucosamine-2-epimerase/N-acetylmannosamine kinase (*GNE* [MIM 603824])[9,10]	enzyme
Nebulin early-onset distal myopathy	nebulin (*NEB* [MIM 161650])[11]	sarcomeric
Miyoshi myopathy type 3 (MMD3 [MIM 613319])	anoctamin 5 (*ANO5* [MIM 608662])[12]	transmembrane

revealed increased affinity for actin. Cell-culture transfection studies with mutant filamin C proteins demonstrated altered nuclear localization and aggregate formation.

Material and Methods

Approvals

All sample collection and experimentation was performed with informed consent from the patients according to approvals given by the University of Western Australia Bioethics Committee or with informed consent from the patients, according to the Declaration of Helsinki.

Skeletal Muscle Pathology

Victorian Family

Collected biopsy tissue was immediately frozen in liquid nitrogen-chilled isopentane and was routinely processed for histology and histochemistry. Immunocytochemical analysis was performed with the following antibodies: dystrophin (Dys1, Dys2, Dys3), dysferlin, myotilin, merosin, titin, sarcoglycans (α, β, γ, δ, and ε), αB-crystallin (Leica Microsystems, Newcastle Upon Tyne, UK), laminin β, laminin γ, and collagen VI (Millipore, MA, USA), with a horseradish peroxidase detection system. Filamin location was determined with the RR90 antibody,[16] followed by incubation with a rabbit anti-mouse IgA secondary and a goat anti-rabbit Alexa Fluor 488 tertiary antibody. Nuclei were labeled with Hoechst.

Italian Family

Muscle biopsy samples were originally analyzed with routine histology and histochemical stainings. After identification of the mutated gene, samples were processed for immunohistochemical analysis with a panel of antibodies against myotilin (Leica Microsystems, Newcastle Upon Tyne, UK), desmin (Biogenex Laboratories, CA, USA), αB-crystallin (Leica Microsystems, Newcastle Upon Tyne, UK), filamin C (Sigma-Alderich, MO, USA), actin (Invitrogen Corporation, CA, USA), and α-actinin (Sigma-Alderich, MO, USA) to assess myofibrillar protein aggregation. The immunohistochemical stainings were made with the BenchMark Immunostainer (Ventana Medical Systems, Arizona, USA) with a peroxidase-based detection kit (Universal DAB Detection Kit, Ventana Medical Systems, Arizona, USA).

Linkage Analysis

Victorian Family

A genome-wide SNP screen was performed on DNA from the Victorian family with the Xba 142.2 10K array system (Affymetrix). Allegro[17] was used to calculate linkage. Pelican 1.2.0[18] created pedigree files, and Alohomora v0.26[19] generated input files for Allegro. Pedcheck[20] was utilized to check for Mendelian errors. Haplotypes were viewed with the program Haplopainter v0.24Beta.[21] LOD scores were calculated with the disease allele frequency set to 1/10,000 and assuming complete penetrance.

Italian Family

Linkage analysis to the *FLNC* region on chromosome 7 was performed with six microsatellite markers (D7S2471, D7S686, D7S2501, D7S2519, D7S2531, D7S1804) distributed over a 6.4 Mb region around *FLNC*. Sets of microsatellite markers for the genes *GNE* (MIM 603824), *MYH7* (MIM 160760), *MYOT* (MIM 604103), *TTN* (MIM 188840), *TPM2* (MIM 190990), *VCP* (MIM 601023), *WDM* (MIM 604454), and *ZASP* (MIM 605906) were also used for genotyping of the samples.

FLNC Sequencing

The entire *FLNC* (NM_001127487.1) transcript was sequenced upon amplification of six overlapping fragments. Template cDNA was synthesized from mRNA extracted from skeletal muscle biopsies of two affected family members from the Victorian family and one control sample. For the Italian family, the N-terminal exons 2–10 of *FLNC* were sequenced from genomic DNA. The primers used for amplifying and sequencing the fragments were designed with the Primer3 software (Table S1, available online). PCR products were sequenced on an ABI3730, automatic DNA sequencer system (Applied Biosystems, Foster City, CA) with the Big Dye Terminator kit and analyzed with Sequencher 4.8 software (Gene Codes Corporation, Ann Arbor, MI).

Mutation Screening in Control Individuals

The c.752T>C (p.Met251Thr) mutation identified in the Victorian family creates a *MaeIII* restriction site not present in the wild-type sequence. *MaeIII* (New England Biolabs) digestion (as per the manufacturer's guidelines) was therefore used to screen DNA samples from unrelated control individuals. We performed screening of controls for the c.577G>A (p.Ala193Thr) mutation identified in the Italian family by sequencing exon 2 of *FLNC* (forward: 5′-AAGAACTTGGCATCTGAGTGG-3′; reverse: 5′-GGTG TGCATTCTGACAACCA-3′).

Cloning of Truncated and Full-Length Filamin C Constructs

Three different regions of *FLNC* were amplified from wild-type and Victorian family patient skeletal muscle cDNA encompassing: (1) the CH1 and CH2 domains, (2) both CH domains and the region between CH2 and immunoglobulin-like (Ig-like) repeat 1, and (3) both CH1 domains and Ig-like repeat 1 (Figure S1 and Table S2). These fragments were cloned into the pET44a or pGEX6P1 vectors to enable prokaryotic expression or the pEGFP-N1 expression vector (Clontech) for eukaryotic expression. The three different p.Met251Thr mutant filamin C fusion proteins localized similarly to one another yet differently to the three wild-type constructs. Therefore, in subsequent experiments, the corresponding longer versions of the ABDs of filamin A and filamin B were also amplified from skeletal muscle cDNA and cloned into pEGFP-N1. The *FLNA* [MIM 300017] and *FLNB* [MIM 603381] mutations and the *FLNC* p.Ala193Thr mutation were introduced by amplification of the template with primers containing the mutant sequence.

A full-length *FLNC* cDNA clone in pEGFP-N3 was obtained in two steps. A fragment encoding domains 15–24 was amplified by PCR from a human skeletal muscle cDNA library (Clontech) and cloned into vector pEGFP-N3 (Table S3). Subsequently, a fragment encoding ABD-d15 was amplified with a *FLNC* cDNA as a template (HP07616-ARi57A02, deposited by Seishi Kato, Research Institute of National Rehabilitation Center for Persons with Disabilities and provided by the RIKEN BioResource Center) and cloned in the partial *FLNC* clone with a unique *BclI* restriction site within the cDNA encoding d15 to obtain a full-length construct. From the above-mentioned mutant *FLNC* ABD and Ig-like repeat 1 constructs, an EcoRI/*AccI* fragment encoding the ABD and part of repeat 1 was purified and used in place of the equivalent wild-type fragment in the full-length *FLNC* clone in pEGFP-N3. This substitution method was used to produce both mutant *FLNC* variants.

Expression and Purification of Recombinant Proteins

Protein expression was performed as described previously.[22] Truncated cDNA fragments were cloned either into the prokaryotic expression vector pET44a, resulting in fusion proteins carrying a C-terminal His_6-NusA tag, or into pGEX-6P1 (Amersham), enabling expression of glutathione S-transferase (GST) fusion proteins. His_6-tagged proteins were expressed in *E. coli* BL21-CodonPlus(DE3)-RIL (Novagen) and purified with the QiaExpress kit as described by the manufacturer (QIAGEN). The Nus-His_6 tag (pET44a) was removed by tobacco etch virus protease (10 μg/ml) cleavage overnight at 16°C. GST-tagged proteins were expressed in *E. coli* and purified on Glutathione-Uniflow Resin columns (Clontech). GST was cleaved from the proteins with PreScission Protease (Amersham) according to the recommendations of the manufacturer. Protein concentrations were determined by densitometric calculation (Odyssey Infrared Imaging System, LI-COR Biosciences GmbH, Bad Homburg).

Biophysical Characterization

Circular dichroism spectroscopy was performed after dialysis of purified proteins against 150 mM sodium phosphate and measurement of the concentration at 280 nm with the extinction coefficient 55,460 $M^{-1}cm^{-1}$. Equal protein quantities of wild-type ABD or both mutant ABDs in 300 μl buffer were added to a 1 mm quartz cuvette, and CD spectra were recorded from 190 nm to 260 nm with a Pistar-180 spectrometer (Applied Photophysics). For differential scanning fluorimetry (Thermofluor) stability assays, 5 μl SYPRO Orange dye (30x, Invitrogen) was added to 10 μl protein sample. Assays were carried out in an IQ5 real-time PCR detection system (Bio-Rad). Temperatures varied from 20°C–95°C with a fluorescence excitation at 470 nm and detection at 555 nm.

Limited Proteolysis

Proteolytic susceptibility was investigated with the endopeptidase thermolysin (Sigma). The protein was diluted to 10 μM (50 mM NaH_2PO_4, 300 mM NaCl, and 250 mM imidazole [pH 8.0]); 10 μg/ml thermolysin was added, and the mixture was incubated at 37°C. At each incubation interval, the reaction was stopped by adding 0.2 vol. 5× SDS sample buffer. The samples were run on a 12% polyacrylamide gel, and band intensities were measured by densitometry.

Cosedimentation Actin-Binding Assay

Muscle actin was purified from acetone powder prepared from chicken breast muscle as described.[23] Cosedimentation assays were performed essentially as described previously.[24] Equal volumes of supernatant and pellet were analyzed by polyacrylamide gel electrophoresis (12% w/v). Gels were stained with Coomassie Brilliant Blue, and protein bands were quantified by densitometry with the Odyssey Imaging System (LI-COR). Ten samples were assayed for each ABD, and the results were combined for hyperbole regression analysis. Calculation of K_d values and definition of the coefficient of correlation were performed with GraphPad Prism (GraphPad Software).

Cell Culture

C2C12 myoblasts, COS7, HEK293, and HeLa cells were resurrected in Dulbecco's Modified Eagle's Medium (DMEM) supplemented with 4 mM L-glutamine (Sigma-Aldrich) and 10% fetal calf serum (GIBCOBRL). Cells were seeded onto coverglass coated with Matrigel (BD Biosciences) and transfected with the pEGFP-N1+FLN vectors with Lipofectamine 2000 (Invitrogen). The following day, the C2C12 cultures were placed into DMEM containing 5% horse serum to promote myotube formation. Cells were fixed 24–48 hr posttransfection in 2% paraformaldehyde, except the C2C12 myotubes, which were fixed between day 5 and 6 of myotube differentiation.

After fixation, cells were washed in PBS and mounted with Hydromount (National Diagnostics). For transfection of the full-length wild-type and mutant filamin C constructs, PtK2, or C2C12 cells were grown, transfected, and stained essentially as described.[16,24] The formation of aggregates after transfection of C2C12 cells with wild-type, p.Met251Thr, and p.Ala193Thr filamin C was characterized by protein distribution and estimation of aggregate number and size in individual cells (n = 110). Cells were visualized and photographed with an Olympus IX71 or a Zeiss Axio Imager M1 microscope equipped for fluorescence and a Biorad MRC 1000/1024 confocal microscope.

Results

Refinement of the Victorian Family Phenotype

Further analysis of the affected members of the Australian family refined the clinical phenotype to identify nine affected and three unaffected individuals available for study. The disease most often started in the third decade of life in the hands and was characterized by thenar muscle weakness leading to reduced grip strength. This was followed by calf muscle weakness beginning around the fourth decade of life and leading to difficulties in running and jumping. Progression to proximal muscles was evident in the fifth decadeof life and usually required a stick for

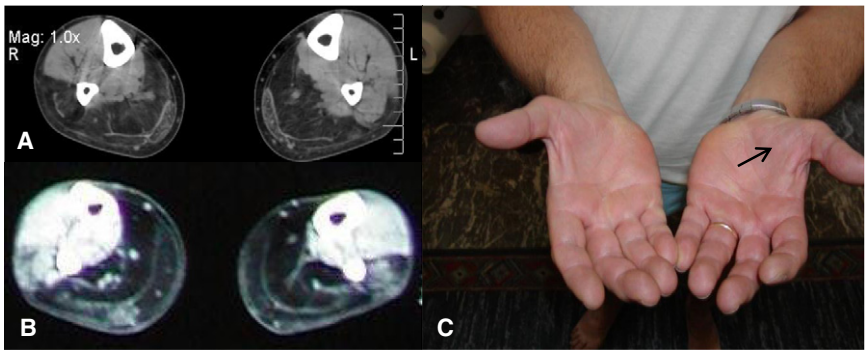

Figure 1. Muscle Wasting in Patients of the Victorian and Italian Distal Myopathy Families

(A) A computed tomography (CT) scan of the lower leg in a 39-year-old female patient from the Victorian family. Severe fatty degeneration of both soleus muscles and right peroneal muscles is evident; there is slightly less involvement of medial and lateral gastrocnemius muscles and radiologically normal anterior compartment and tibialis posterior muscles.

(B) CT imaging of the lower legs in the Italian male patient. Severe fatty degeneration of soleus and gastrocnemii muscles are evident with less severe changes in peroneal muscles and sparing of anterior compartment and tibialis posterior muscles.

(C) Marked atrophy of thenar muscles in patient III:3 from the Italian family (marked by arrow).

walking in the sixth decade of life. The distribution of the most affected calf muscles was easily shown by muscle imaging as a striking selective fatty degeneration of posterior compartment muscles in the lower leg (Figure 1). Early changes in thigh muscles are fatty degeneration of semimembranosus and semitendinosus muscles and later involvement of all hamstring muscles, the adductor magnus, and, even later, vastii muscles of the quadriceps. Electron microscopy studies on one muscle biopsy did not demonstrate any pathological features. There are no manifestations of respiratory or cardiac insufficiency even at an advanced age of more than 75 years.

Muscle Pathology in the Victorian Family

Muscle biopsies were reviewed on four family members with a spectrum of findings determined (Figure S2). Necrosis, vacuoles, inclusions, regeneration, and inflammation were not observed. The array of antibodies showed no major reactivity outside that of a normal muscle, and electron microscopy did not show myofibrillar pathology.

Patient 1 biopsies, taken from the left bicep at 54 years of age, showed nonspecific changes and a very occasional rounded atrophic muscle fiber.

Patient 2 biopsies collected at 44 years of age, were of end-stage myopathic muscle with extensive fatty atrophy. Residual fibers showed fiber size variation and atrophic rounded fibers of both fiber types. Internal nuclei and fiber splitting were not seen. There were no ragged red fibers or cytochrome oxidase-depleted fibers, and there was no evidence of any change in distribution of the oxidative enzymes. The array of antibodies showed scant internalization of dysferlin, αB crystallin in a few fibers, and fine granular myotilin deposits within the cell.

Patient 3 biopsies taken from the left vastus medialis at 76 years of age showed features of a myopathy and minor variation in myofiber size in both fiber types. There was no increase in the number of internal nuclei, and there were no split fibers. Scattered fibers showed an irregular flocculent pale eosinophilic material within the cytoplasm, but no vacuoles were seen that appeared to correlate with areas lacking oxidative enzyme activity. Gomori Masson stains showed scant fibers with subsarcolemmal accumulation of basophilic material. Many fibers showed a moth-eaten appearance on oxidative enzyme stains.

Patient 4 biopsies taken from the left soleus at 47 years of age showed a myopathic pattern of patchy variation in fiber size and scattered tiny atrophic fibers that appeared eosinophilic and were of both fiber types. The muscle appeared to be type 1 dominant. There was a focal increase in interstitial fibrosis, a focal minor elevation in internal nuclei, and scant degenerating fibers. There was an extensive moth-eaten appearance to fibers, a loss of oxidative enzyme stains, and patchy irregular cytochrome oxidase negativity. The array of antibodies showed minor patchy loss of surface dysferlin but no other evident change in the distribution of the fibers.

Identification of an Italian Family

The refinement of the clinical and muscle imaging phenotype in the Australian family facilitated the identification of the same phenotype in a family from Italy from among the distal myopathy families who had been referred to us for molecular genetic evaluation. There are four known affected members in the pedigree (Figure 2).

All three available patients experienced reduced finger skills and running performance at approximately 30 years of age. Slow progression to the proximal lower limb muscle occurred over the following 20 years, and there was evident atrophy of the hand muscles (Figure 1), an inability to squat, and use of a stick for walking by age 60. Creatine kinase levels were only slightly elevated and ranged from 1.5× to 2.5× the normal upper limit in all three patients examined. There were no respiratory features evident in the examined family members, but two out of the four patients had cardiomyopathy.

Muscle Pathology in the Italian Family

Muscle pathology in the Italian family was derived from a less affected deltoid muscle biopsy showing nonspecific changes such as a variation of fiber size with scattered atrophic fibers and an increase of internal nuclei but no fiber

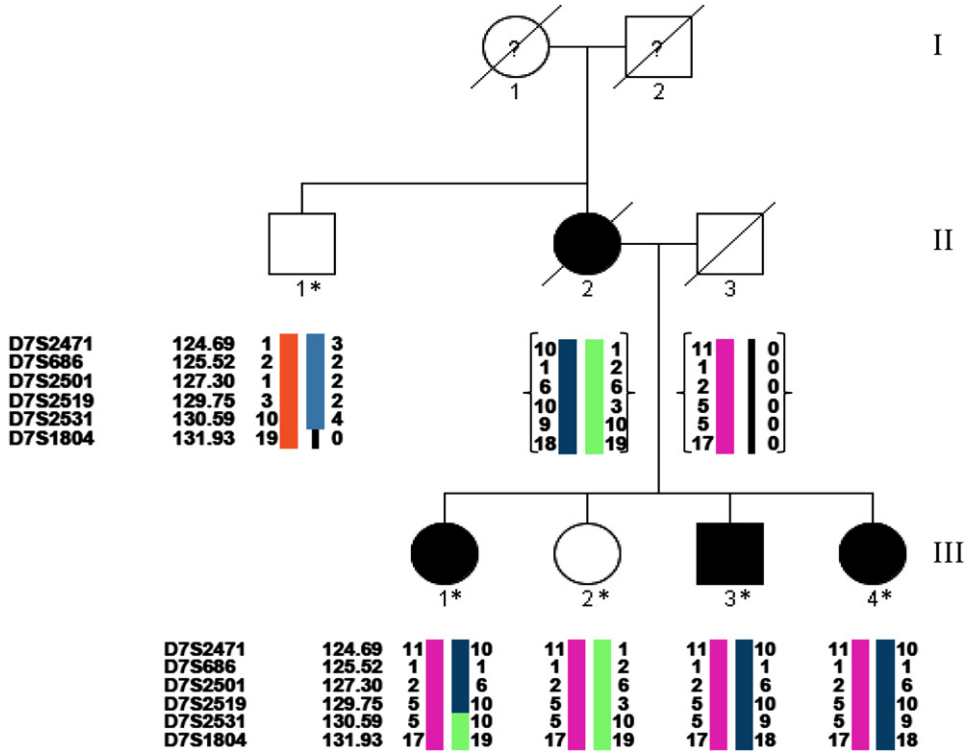

Figure 2. Pedigree of the Italian Family
Pedigree of the Italian family with distal myopathy identified in this study. The segregation of haplotypes around *FLNC* chromosome 7 are represented by colored bars. Samples with DNA available for study are marked with an asterisk (*). Inferred haplotypes are enclosed with brackets. A recombination between microsatellites D7S2519 and D7S2531 was observed in individual III:1. *FLNC* is located between markers D7S2501 and D7S2519.

necrosis or rimmed vacuolar changes. The results of immunohistochemical analysis with a panel of antibodies revealed that the characteristic protein aggregations, as observed in myofibrillar myopathology, were not present in the sample from the Italian family (individual III:1) (Figure S3).

Linkage Studies

In view of the refined clinical phenotype in the Victorian family, especially in relation to the age at onset, all members of the youngest generation of the Victorian family were classified as unknown for the purposes of linkage analysis. In addition, all family members who could not be re-examined were also classified as unknown. Thus, nine affected and three unaffected family members were included in the linkage analysis. Genome-wide SNP analysis with the Xba 142.2 10K array system (Affymetrix) identified a single significant multipoint LOD score of 3.3 on chromosome 7 (Figure S4). The linkage region encompassed 18.6 Mbp between SNPs rs754920 (128,468,162 bp) and rs1406288 (147,110,180 bp).

The smaller Italian family was shown to be compatible with linkage to the same region by analysis of the microsatellites D7S2471, D7S686, D7S2501, D7S2519, D7S2531, and D7S1804 distributed over a 7.2 Mb region. The linked region encompassed less than 6 Mb of this area between markers D2S2471 and D67S2531 (Figure 2).

FLNC Mutation Screening

The 18.6 Mbp linkage region in the Victorian family contained an estimated 151 genes. The gene for filamin C (*FLNC*) was considered the most likely candidate gene within the linkage region on the basis of its role in skeletal muscle structure and function and the fact that mutations in this gene had previously been associated with myofibrillar myopathy.[25,26] The entire *FLNC* cDNA from two affected family members of the Victorian family was sequenced. A thymine to cytosine transition mutation resulting in a c.752T>C (ATG > ACG; p.Met251Thr) mutation was detected in exon 4 (Figure 3). The mutation segregated with the disease in the family giving a two-point LOD score of 3.31. The mutation was not present in 200 unrelated control individuals (400 chromosomes) screened.

In the Italian family, sequencing the N-terminal exons 2–10 of *FLNC* from genomic DNA identified a c.577G>A (GCC > ACC; p.Ala193Thr) mutation in exon 2 (Figure 3). This mutation segregated with the disease in the family and was not seen in 102 control individuals (204 chromosomes).

Biophysical Characterization and Actin-Binding Assay

In order to investigate potential alterations of biophysical and biochemical properties caused by the described mutations, we first analyzed the secondary structure by

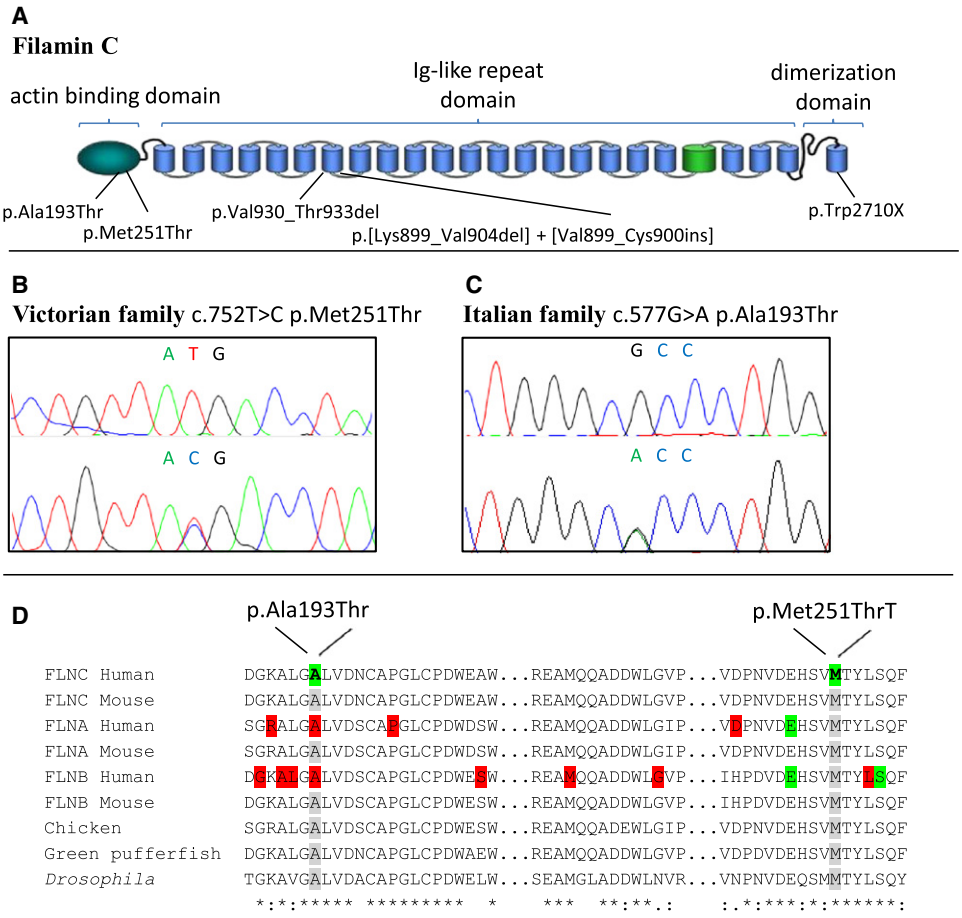

Figure 3. Mutations in the Filamin C Protein

(A) The filamin C protein with the position of the two mutations identified in this report marked on the ABD. The mutations in Ig-like repeats 7 and 24 responsible for myofibrillar myopathy [MIM 609524] are also indicated.

(B) Chromatogram showing the c.752T>C heterozygous missense mutation resulting in a p.Met251Thr amino acid change identified in the Victorian family.

(C) Chromatogram showing the c.577G>A missense mutation resulting in a p.Ala193Thr amino acid change identified in the Italian family.

(D) Multiple sequence alignment of homologous ABDs with known mutations highlighted in red, mutations investigated in transient transfection experiments in cell culture in this report highlighted in green, and the position of the mutations identified in this study highlighted in gray.

performing circular dichroism spectroscopy of bacterially expressed ABDs. In accordance with the established crystal structures of filamin ABDs, both the wild-type and the mutant proteins exhibited a high proportion of α helices, as evidenced by two minima in the spectrum at 208 and 222 nm and a maximum at 200 nm. The spectrum of the p.Ala193Thr mutant was essentially identical to the wild-type protein, whereas the p.Met251Thr mutant showed slightly decreased ellipticity at the 200 nm and 222 nm peaks (Figure 4A).

To test whether these alterations would translate into changes of protein stability, we performed a fluorescence-based thermal shift assay (Thermofluor) of p.Met251Thr and p.Ala193Thr in comparison to the wild-type filamin C ABD. This revealed a melting temperature of 59.3°C for the wild-type ABD, whereas the p.Met251Thr and p.Ala193Thr mutant ABDs showed decreased average melting temperatures of 51°C and 52.3°C, respectively. A limited thermolysin protease digestion was performed as a second test of protein stability. At 37°C this assay did not reveal any significant differences between the wild-type, the p.Met251Thr, and the p.Ala193Thr mutant ABDs.

To further analyze the binding capacities of wild-type and mutant ABDs to F-actin in a quantitative manner, we performed actin filament cosedimentation assays. All ABDs clearly bound to and cosedimented with skeletal muscle F-actin in a dose-dependent manner (Figure 4B). Whereas the wild-type ABD had a calculated K_d value of 8.2 μM, the K_d of the p.Ala193Thr mutant was moderately elevated (5.7 μM), and the p.Met251Thr mutant demonstrated a highly increased actin-binding activity with a K_d of 3.7 μM (Figure 4C). As a comparison, the K_d of the ABDs of filamin A and filamin B was reported to be 17μM and 7.0 μM, respectively.[27,28]

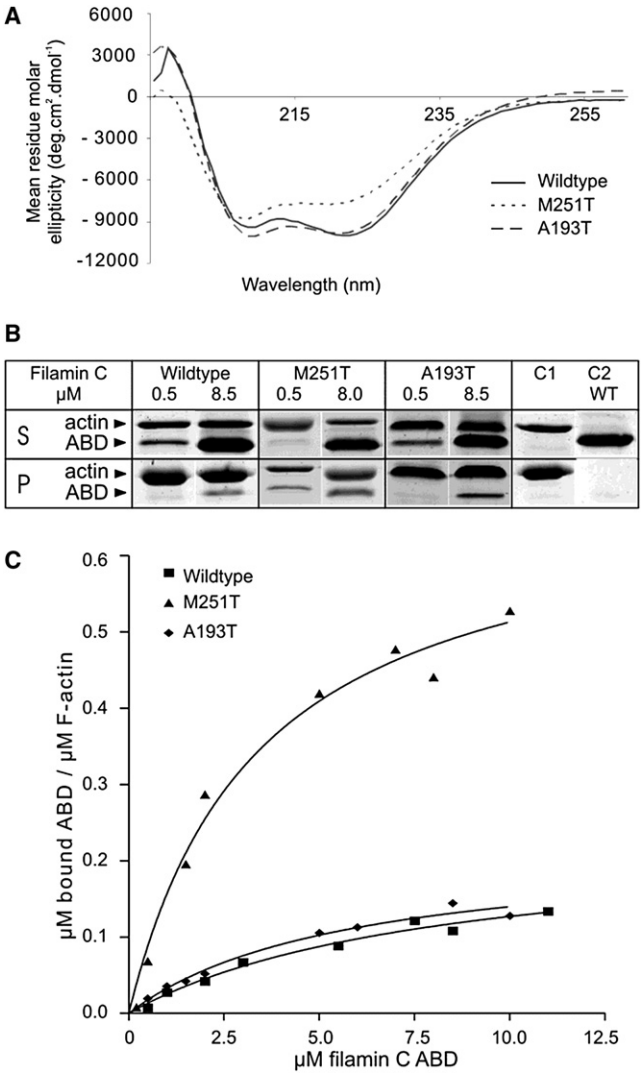

Figure 4. Protein Foldedness and Actin-Binding Assays
(A) Circular dichroism spectroscopy in the far UV range was performed with purified, bacterially expressed wild-type and mutant filamin ABD constructs. The mean residue ellipticity (MRE) shows two minima in the spectrum at 208 and 222 nm and a maximum at 200 nm, typical for the presence of a high proportion of α helices. Note that the spectra of the wild-type and p.Ala193Thr mutant are almost identical, whereas the MRE of the p.Met251Thr mutant shows a slightly decreased ellipticity compared to the ellipticity of the p.Ala193Thr and wild-type constructs.
(B and C) Actin-binding assays of filamin C wild-type and mutant ABDs. (B) The results of high-speed F-actin cosedimentation assays. The numbers on top of each lane indicate the amount of recombinant ABD added to 5 μM actin. Given are the supernatant (S) and pellet (P) fractions. The following abbreviations are used: C1, control without ABD; C2, control without actin. (C) Binding curves with F-actin. The mutant proteins exhibited increased actin-binding activity, represented by a change in dissociation constant (Kd) to 3.7 μM for p.Met251Thr and 5.7 μM for p.Ala193Thr when compared to the wild-type filamin C (Kd = 8.2 μM).

Analysis of Wild-Type and Mutant Filamins A, B, and C in Cell Culture

Three different length amino terminal constructs of wild-type, p.Met251Thr, or p.Ala193Thr filamin C encompassing the ABD, the ABD and the adjacent linker, or the ABD in addition to the first Ig-like repeat were cloned into a pEGFP-N1 vector and transfected into C2C12, COS-7 (Figure S5), HEK293, and HeLa cells. By fluorescence and confocal microscopy, several gross morphological differences were observed in C2C12 cells expressing the three mutant fusion proteins in comparison to those expressing any of the three wild-type fusion proteins. These included an increased presence of stress fibers, increased length and intricacy of projections from the cell, and lower intensity of fluorescent signal in the nucleus of the mutant as compared to the nucleus of the wild-type (Figure S6).

Additionally, all three truncated filamin C (WT)-EGFP fusion proteins localized to both the nuclei and sarcoplasm of C2C12 cells, whereas the filamin C-(p.Met251Thr)-EGFP fusion proteins showed significantly diminished nuclear localization. This disparity in nuclear localization between wild-type and p.Met251Thr filamin C ABD was found in all transfected cell lines, including COS-7 (Figure S5), HEK293, and HeLa cells (not shown).

Transfection of COS-7 (Figure S5), HEK293, and HeLa cells with wild-type and mutant filamin A (NM_001110556.1) (c.760G>A, p.Glu254Lys) and filamin B (NM_001164317.1) (c.679G>A, p.Glu227Lys and c.703T>C, p.Ser235Pro) constructs, equivalent to the longest of the three filamin C constructs (ABD and repeat 1), demonstrated a similar effect of reduced nuclear localization of each the mutant fusion proteins compared to nuclear localization in the wild-type fusion proteins. In contrast, the fusion proteins containing the Italian family mutation in *FLNC* (p.Ala193Thr) showed a similar localization pattern to the wild-type in COS-7 cells (Figure S5) and all further cell lines examined (C2C12, HEK293, and HeLa cells).

To analyze the effect of the expression of both filamin C mutations in PtK2 epithelial cells and C2C12 myoblasts, we transiently transfected these cells with constructs encoding full-length wild-type or mutant filamin C. In PtK2 as well as C2C12 cells, expression of wild-type filamin C resulted in an association of the EGFP fusion protein with stress fibers (Figures 5A and 5D). The variants p.Met251Thr and p.Ala193Thr also associated with stress fibers (Figures 5B, 5C, 5E, and 5F).Otherwise, expression of both mutants, but not the wild-type protein, resulted in the development of protein aggregates in up to 100% of the transfected cells (Figures 5B, 5C, 5E, and 5F). Costaining with phalloidin revealed that these aggregates, especially the larger ones, also contained F-actin (Figures 5B, 5C, 5E, and 5F). Interestingly, the majority of the cells transfected with the p.Met251Thr mutant contained few large aggregates, whereas the aggregates in cells transfected with the p.Ala193Thr mutant were numerous and small (Table 2).

Discussion

We previously described a large family from Victoria in Australia with a distal myopathy phenotype, which did not link to any of the known distal myopathy loci.[14] The

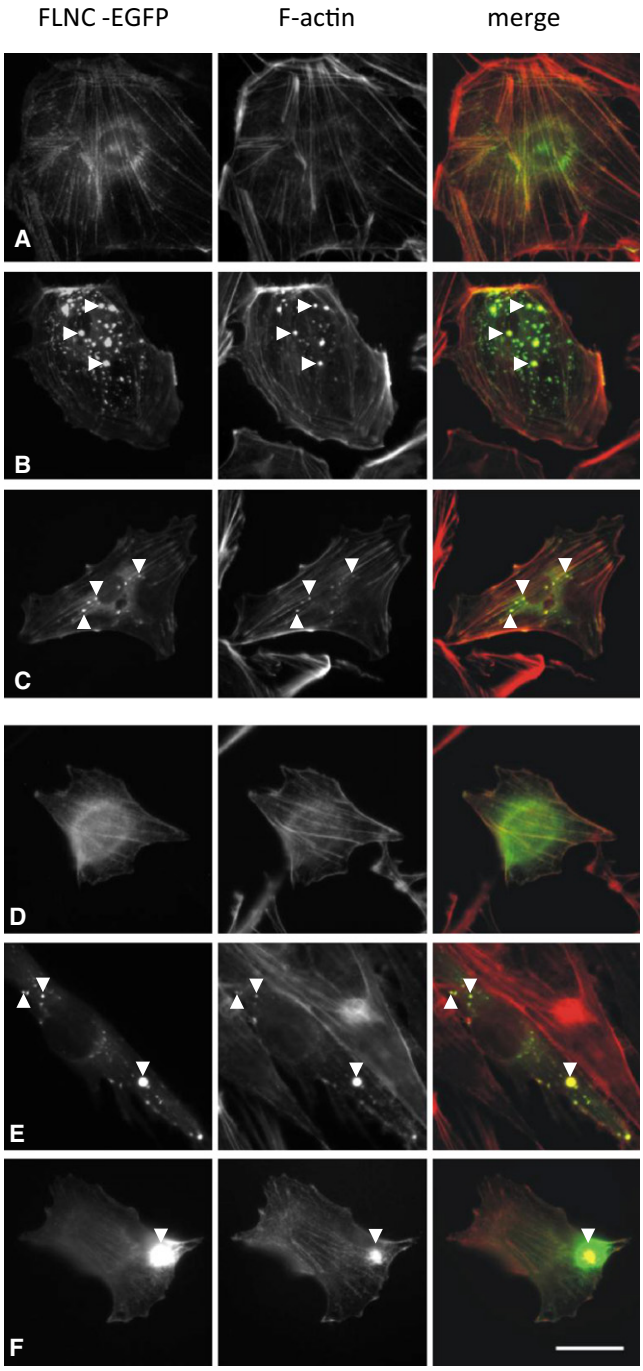

Figure 5. Transient Transfection of Full-Length Wild-Type or Mutant Filamin C in PtK2 and C2C12 Cells
Shown are immunoflouorescence micrographs of PtK2 (A, B, and C) or C2C12 (D, E, and F) cells transfected with full-length, EGFP-tagged, wild-type (A and D) mutant p.Ala193Thr (B and E) or mutant p.Met251Thr (C and F) filamin C. Note that in both cell types all EGFP fusion proteins are targeted to stress fibers. Only the mutant constructs are additionally localized either in numerous differentially sized aggregates (B, C, and E) or in one or a few large aggregates. (F) Note that primarily the larger aggregates (arrowheads) are costained by F-actin. The scale bar represents 20 μm.

distal myopathy in this family is characteristic and distinguishable clinically from other distal myopathies by the first symptom of thenar muscle weakness and later by posterior calf muscle involvement. On the muscle biopsy, there was an absence of rimmed vacuoles or marked myofibrillar myopathy changes. The characterization of the clinical phenotype in the Victorian family allowed the identification of a second Italian family with a similar distal myopathy. Genome-wide linkage analysis of the Victorian family identified one significant linkage region on chromosome 7. *FLNC* was considered the most likely candidate gene in the linkage region. Analysis of cDNA from affected family members identified a c.752T>C (p.Met251Thr) *FLNC* mutation that is located in the N-terminal ABD of the protein product. The p.Met251Thr variant segregated with the disease in the family but was not seen in 400 control chromosomes. A c.577G>A (p.Ala193Thr) mutation was subsequently identified within the filamin C ABD in the Italian family.

The Filamin Protein Family

Filamin C is a member of the three-member filamin protein family. Filamin C expression is mainly restricted to skeletal muscle and the heart in the adult. The other two filamins, filamin A and filamin B, are ubiquitously expressed.[29] The three filamins share the same basic structure of an N-terminal ABD and consist of two calponin homology (CH) domains, followed by 24 Ig-like repeats[30] that include two hinge regions at the 15th and 23rd repeats and a C-terminal dimerization domain (repeat 24).[31] The filamins are actin cross-linking proteins that play a role in stabilizing bundles of parallel actin filaments or networks.[32] The ability of filamins to efficiently cross-link actin filaments results from dimerization of two filamin monomers at the dimerization domain.[33] The filamins are involved in multiple functions, including control of cell structure, cell signaling, nuclear signaling, and motion.[29,34] Filamin C in skeletal muscle localizes mainly to the Z disk, where it binds myopodin,[35] myotilin,[16] and FATZ.[36] A small fraction of the protein is localized to the sarcolemma, where it binds sarcoglycans[37] and to the myotendinous junction.[16] Filamin C also plays a role in myogenesis[38] and is a substrate of the muscle-specific calpain 3.[39]

Known Filamin C Mutations

A mutation in the ABD of filamin C has not previously been identified. Three disease-causing mutations have previously been described in filamin C, all associated with a typical myofibrillar myopathy phenotype [MIM 609524].[25,26,40] The first reported *FLNC* disease-causing variant was a p.Trp2710X nonsense mutation occurring within the dimerization domain at the C-terminal end of the protein[25] that alters the dimerization properties of the protein. Curiously, the other two known mutations are both in the seventh Ig-like repeat of filamin C, a 12-nucleotide deletion (c.2997_3008del) that removes four amino acids (p.Val930_Thr933del)[26] and a complex

Table 2. Analysis of Protein Distribution and Aggregation of Full-Length Wild-Type and Mutant Filamin C-EGFP Fusion Proteins in Transfected C2C12 Cells

	No Aggregates, Fusion Proteins Associated with Stress Fibers	Aggregates, Fusion Proteins Associated With Stress Fibers	1–3 Large Aggregates	> 3 Small Aggregates
Wild-type	100%	–	–	–
p.Met251Thr	–	100%	73%	27%
p.Ala193Thr	1%	99%	3%	96%

deletion-insertion mutation (c.2695_2712delinsGTTTGTT) that removes six amino acids and inserts two amino acids in frame (p.[Lys899_Val904 del]+[Val899_Cys900ins]).[40] The functional consequences of the latter two mutations await further studies. These three previously reported mutations are associated with a different pattern of muscle involvement on MRIs and more proximal weakness[25,26,40] than was observed in the two families described in this paper. Although one myofibrillar myopathy patient had reported distal weakness of one calf muscle,[25] this condition is still classified as a proximal muscle disease, whereas the condition described here is a distal myopathy phenotype.

The muscle pathology associated with the previously described filamin C mutations is, similar to all other myofibrillar myopathies, characterized by a marked Z disk disintegration and accumulation of myofibrillar proteins.[41,42] The presence of nemaline bodies, as seen in the previously described patients, is a characteristic feature of filamin myofibrillar myopathy.[25,26] Neither florid accumulation of myofibrillar proteins nor Z disk disintegration characteristic of the myofibrillar myopathies was seen in any of the muscle biopsies from the two families presented here.

Thus, muscle pathology findings also support a different disease mechanism caused by mutations in the ABD of filamin C. Table S4 presents a comparison of the phenotypes and the pathological features of the two conditions.

Other Filamin and Related Protein Diseases

The ABD of all filamins consists of two calponin homology domains (CH1 and CH2). Each CH domain contains four major helices (A, C, E, and G), other minor helical segments, and nonhelical linkers.[28,43,44] This double-CH domain ABD form is shared by a number of other actin-binding proteins, including α-actinin, dystrophin, and utrophin.[28,44]

The two mutations identified in the distal myopathy families in the present study, p.Ala193Thr and p.Met251Thr, are both located in the CH2 domain of the ABD. A protein sequence alignment of the CH2 domain in filamin C, filamin A, and filamin B and the orthologous proteins in green pufferfish, chicken, and *Drosophila* shows a 100% conservation of both the p.Ala193 and p.Met251 residues (Figure 3). The two residues are thus highly conserved throughout evolution and provide further weight to the conclusion that these are the disease-causing mutations in the two families.

Although mutations have not previously been reported in the ABD of filamin C, mutations have been described in the ABD of filamins A and B. Mutations in the ABD of filamin A result in otopalatodigital syndrome types 1 (OPD1 [MIM 311300]) and 2 (OPD2 [MIM 304120]), frontometaphyseal dysplasia (FMD [MIM 305620]), and Melnick-Needles syndrome (MNS [MIM 309350]).[45] Mutations in the ABD of filamin B result in autosomal-dominant Larsen syndrome (LRS1 [MIM 150250]), atelosteogenesis types I (AOI [MIM 108720]) and III (AOIII [MIM 108721]), and boomerang dysplasia (MIM 112310).[46] The homolog of the filamin C p.A193 residue mutated in the Italian distal myopathy family is mutated in filamin A in OPD2 (p.Ala200Ser)[45] and in filamin B in AOI (p.Ala173Val).[47] A mutation (p.Tyr231Asn) in dystrophin within the CH2 domain results in Becker muscular dystrophy [MIM 300376],[48] and mutations in the CH2 domain of α-actinin 4 (*ACTN4* [MIM 604638]) cause focal segmental glomerulosclerosis (FSGS1 [MIM 603278]).[49]

Pathomechanisms of Filamin Mutations

It is well known that mutations in different domains of filamin A and filamin B cause different diseases.[45,47] Our results suggest similar effects for mutations in different parts of filamin C, because the ABD mutations we have identified in the Victorian and Italian families result in a different clinical and pathological phenotype to the myofibrillar myopathy phenotypes caused by mutations elsewhere in the gene.

The p.Trp2710X dimerization domain mutation destroys the ability of the protein to dimerize and cross-link actin, leading to the formation of aggregates of filamin and its binding partners, desmin, myotilin, and sarcoglycans.[22] The Ig-like repeat mutations are also associated with accumulation of filamin and the other proteins that normally accumulate in myofibrillar myopathies; however, the exact mechanisms are uncertain.[26,40]

Our actin-binding studies demonstrate increased actin-binding affinity of the two distal ABD-filaminopathy mutations in filamin C. This is similar to previous results for disease-causing mutations in the actin-binding domains of filamins A[43] and B[28] and also for mutations in the ABD of α-actinin-4 that cause focal segmental glomerulosclerosis.[49]

The following mechanism might explain differences in binding of wild-type and mutant ABDs to F-actin: the N-terminal or CH1 domain by itself is able to bind actin

filaments, whereas the CH2 domain alone cannot, but F-actin binding is increased 10-fold when both domains are present.[50,51] Thus, although the CH2 domain does not possess specific F-actin-binding activity, it contributes to the binding affinity of the ABD as a whole. The current model of α-actinin ABD binding to actin filaments suggests that the presence of CH2 provides steric hindrance to the binding of F-actin and acts as a negative regulator of the interaction. Opening of the CH1-CH2 interface is therefore required for binding.[52] The C-terminal helix of the CH2 domain is involved in a number of predominantly hydrophobic interactions with the CH1 domain, stabilizing in this way the closed conformation of the ABD. The amino acid Met251 resides in this C-terminal helix and plays an important role in stabilizing the interdomain interaction interface. The p.Met251Thr mutation changes the hydrophobic methionine into a hydrophilic threonine and results in decreased interdomain interaction and overall stability of the ABD, as shown by the thermal stability assays. Although this mutation does not alter the secondary structure significantly, it does increase the binding affinity to F-actin because of destabilization of the CH1-CH2 interaction that facilitates the opening of the ABD required to remove the steric clash occurring with F-actin occurring in the closed conformation. In contrast, the p.Ala193Thr mutant directly affects the CH2 subdomain, in proximity to the actin-binding helix C′, and causes a slight alteration of its binding properties. These observations are consistent with filamin B mutations within the actin-binding domain that demonstrate an increased level of actin-binding activity despite minimal structural changes to the protein.[28]

In our transient transfection experiments with the N-terminal constructs, the most obvious difference between wild-type and mutant ABD domains expressed on their own was in the nuclear targeting. This was seen for the p.Met251Thr filamin C mutant and the filamin A (p.Glu254Lys) and filamin B (p.Glu227Lys and p.Ser235Pro) mutants but not for the p.Ala193Thr filamin C mutation. Filamin A C-terminal fragments are known to enter the nucleus and play a role in transcription regulation, including androgen receptor transport into the nucleus.[53–56] The role of filamin C in signal transduction, myogenesis, and muscle regeneration[38,57] suggests a role for it in the nucleus. The results of our overexpression of the ABDs might support a role for filamin C in the nucleus, but the physiological relevance of the finding is uncertain. In addition, the fact that the effect on nuclear localization was not seen for the p.Ala193Thr filamin C mutation suggests that the reduced nuclear localization of the mutant is not primarily responsible for the disease, and the disease is most likely caused in some way by the increased affinity for actin.

Transient expression of full-length mutant ABD-filamins results in aggregation of the expressed proteins together with F-actin, an effect that is not observed upon transfection of the wild-type protein, confirming that the aggregation is caused by the mutations. In corroboration with the in vitro actin-binding data, both mutant proteins and wild-type filamin C all associate with stress fibers. The increased affinity of the mutants for F-actin is obviously sufficient for the aggregation of the mutant proteins together with F-actin. However, in the muscle biopsies of the patients carrying this mutation, no protein aggregates were found, which clearly differentiates this disease from the filamin myopathies described thus far. Possibly the higher expression levels of the mutant protein in transfected cells compared to the expression levels in muscle fibers or the absence of wild-type filamin C in the transfected cells is the reason for this discrepancy.

Conclusions

The finding that mutations within the ABD of *FLNC* result in the distal myopathy in two different families we describe adds understanding to filamin C biology and suggests a different patient cohort should be screened for *FLNC* mutations. All known *FLNC* mutations cause adult-onset muscle disease. Whereas a partial ablation of both *FLNC* alleles results in severe defects in myogenesis and neonatal lethality in mice,[38] the heterozygous *FLNC* mutations found thus far in patients do not seem to greatly affect muscle biology. Our data most strongly support that the disease mechanism, similar to the disease mechanism for ABD mutations in filamins A and B, involves increased affinity for actin. Further work is required to fully understand the pathobiology of distal ABD-filaminopathy.

Supplemental Data

Supplemental Data include six figures and four tables and can be found with this article online at http://www.cell.com/AJHG/.

Acknowledgments

N.G.L. was supported by an Australian National Health and Medical Research Council (NH&MRC) Fellowship (403904); K.J.N. and G.R. by NH&MRC Project Grant 403941. D.O.F. was supported by grants from the German Research Foundation (FOR1228 and FOR1352). D.O.F. and P.F.M.v.d.V. are members of the German muscular dystrophy network (MD-NET 2) funded by the German Ministry of Education and Research (BMBF). K.D.-C. acknowledges support from the Austrian Science Fund (Doctoral Program W1221 Structure and Interaction of Biological Macromolecules). The authors acknowledge the facilities and scientific and technical assistance of the Australian Microscopy and Microanalysis Research Facility at the Centre for Microscopy, Characterisation and Analysis, The University of Western Australia, a facility funded by the university, state, and commonwealth governments. B.U. was supported by the Sigrid Juselius Foundation, the Finnish Academy Foundation, and the Folkhälsan Research Foundation.

Received: February 10, 2011
Revised: April 24, 2011
Accepted: April 29, 2011
Published online: May 26, 2011

Web Resources

The URLs for data presented herein are as follows:

Online Mendelian Inheritance in Man (OMIM), http://www.omim.org

Primer 3 software, http://frodo.wi.mit.edu/primer3/

References

1. Udd, B. (2007). Molecular biology of distal muscular dystrophies—sarcomeric proteins on top. Biochim. Biophys. Acta *1772*, 145–158.
2. Udd, B. (2009). 165th ENMC International Workshop: Distal myopathies 6-8th February 2009 Naarden, The Netherlands. Neuromuscul. Disord. *19*, 429–438.
3. Hackman, P., Vihola, A., Haravuori, H., Marchand, S., Sarparanta, J., De Seze, J., Labeit, S., Witt, C., Peltonen, L., Richard, I., and Udd, B. (2002). Tibial muscular dystrophy is a titinopathy caused by mutations in TTN, the gene encoding the giant skeletal-muscle protein titin. Am. J. Hum. Genet. *71*, 492–500.
4. Meredith, C., Herrmann, R., Parry, C., Liyanage, K., Dye, D.E., Durling, H.J., Duff, R.M., Beckman, K., de Visser, M., van der Graaff, M.M., et al. (2004). Mutations in the slow skeletal muscle fiber myosin heavy chain gene (MYH7) cause laing early-onset distal myopathy (MPD1). Am. J. Hum. Genet. *75*, 703–708.
5. Griggs, R., Vihola, A., Hackman, P., Talvinen, K., Haravuori, H., Faulkner, G., Eymard, B., Richard, I., Selcen, D., Engel, A., et al. (2007). Zaspopathy in a large classic late-onset distal myopathy family. Brain *130*, 1477–1484.
6. Senderek, J., Garvey, S.M., Krieger, M., Guergueltcheva, V., Urtizberea, A., Roos, A., Elbracht, M., Stendel, C., Tournev, I., Mihailova, V., et al. (2009). Autosomal-dominant distal myopathy associated with a recurrent missense mutation in the gene encoding the nuclear matrix protein, matrin 3. Am. J. Hum. Genet. *84*, 511–518.
7. Liu, J., Aoki, M., Illa, I., Wu, C., Fardeau, M., Angelini, C., Serrano, C., Urtizberea, J.A., Hentati, F., Hamida, M.B., et al. (1998). Dysferlin, a novel skeletal muscle gene, is mutated in Miyoshi myopathy and limb girdle muscular dystrophy. Nat. Genet. *20*, 31–36.
8. Bashir, R., Britton, S., Strachan, T., Keers, S., Vafiadaki, E., Lako, M., Richard, I., Marchand, S., Bourg, N., Argov, Z., et al. (1998). A gene related to Caenorhabditis elegans spermatogenesis factor fer-1 is mutated in limb-girdle muscular dystrophy type 2B. Nat. Genet. *20*, 37–42.
9. Eisenberg, I., Avidan, N., Potikha, T., Hochner, H., Chen, M., Olender, T., Barash, M., Shemesh, M., Sadeh, M., Grabov-Nardini, G., et al. (2001). The UDP-N-acetylglucosamine 2-epimerase/N-acetylmannosamine kinase gene is mutated in recessive hereditary inclusion body myopathy. Nat. Genet. *29*, 83–87.
10. Kayashima, T., Matsuo, H., Satoh, A., Ohta, T., Yoshiura, K., Matsumoto, N., Nakane, Y., Niikawa, N., and Kishino, T. (2002). Nonaka myopathy is caused by mutations in the UDP-N-acetylglucosamine-2-epimerase/N-acetylmannosamine kinase gene (GNE). J. Hum. Genet. *47*, 77–79.
11. Wallgren-Pettersson, C., Lehtokari, V.L., Kalimo, H., Paetau, A., Nuutinen, E., Hackman, P., Sewry, C., Pelin, K., and Udd, B. (2007). Distal myopathy caused by homozygous missense mutations in the nebulin gene. Brain *130*, 1453–1455.
12. Bolduc, V., Marlow, G., Boycott, K.M., Saleki, K., Inoue, H., Kroon, J., Itakura, M., Robitaille, Y., Parent, L., Baas, F., et al. (2010). Recessive mutations in the putative calcium-activated chloride channel Anoctamin 5 cause proximal LGMD2L and distal MMD3 muscular dystrophies. Am. J. Hum. Genet. *86*, 213–221.
13. Welander, L. (1951). Myopathia Sistalis Tarda Hereditaria. Acta Med. Scand. *141* (*Suppl 265*), 7–124.
14. Williams, D.R., Reardon, K., Roberts, L., Dennet, X., Duff, R., Laing, N.G., and Byrne, E. (2005). A new dominant distal myopathy affecting posterior leg and anterior upper limb muscles. Neurology *64*, 1245–1254.
15. Mastaglia, F.L., Lamont, P.J., and Laing, N.G. (2005). Distal myopathies. Curr. Opin. Neurol. *18*, 504–510.
16. van der Ven, P.F.M., Obermann, W.M.J., Lemke, B., Gautel, M., Weber, K., and Fürst, D.O. (2000). Characterization of muscle filamin isoforms suggests a possible role of γ-filamin/ABP-L in sarcomeric Z-disc formation. Cell Motil. Cytoskeleton *45*, 149–162.
17. Gudbjartsson, D.F., Jonasson, K., Frigge, M.L., and Kong, A. (2000). Allegro, a new computer program for multipoint linkage analysis. Nat. Genet. *25*, 12–13.
18. Dudbridge, F., Carver, T., and Williams, G.W. (2004). Pelican: Pedigree editor for linkage computer analysis. Bioinformatics *20*, 2327–2328.
19. Rüschendorf, F., and Nürnberg, P. (2005). ALOHOMORA: A tool for linkage analysis using 10K SNP array data. Bioinformatics *21*, 2123–2125.
20. O'Connell, J.R., and Weeks, D.E. (1998). PedCheck: A program for identification of genotype incompatibilities in linkage analysis. Am. J. Hum. Genet. *63*, 259–266.
21. Thiele, H., and Nürnberg, P. (2005). HaploPainter: A tool for drawing pedigrees with complex haplotypes. Bioinformatics *21*, 1730–1732.
22. Löwe, T., Kley, R.A., van der Ven, P.F.M., Himmel, M., Huebner, A., Vorgerd, M., and Fürst, D.O. (2007). The pathomechanism of filaminopathy: Altered biochemical properties explain the cellular phenotype of a protein aggregation myopathy. Hum. Mol. Genet. *16*, 1351–1358.
23. Spudich, J.A., and Watt, S. (1971). The regulation of rabbit skeletal muscle contraction. I. Biochemical studies of the interaction of the tropomyosin-troponin complex with actin and the proteolytic fragments of myosin. J. Biol. Chem. *246*, 4866–4871.
24. Pacholsky, D., Vakeel, P., Himmel, M., Löwe, T., Stradal, T., Rottner, K., Fürst, D.O., and van der Ven, P.F.M. (2004). Xin repeats define a novel actin-binding motif. J. Cell Sci. *117*, 5257–5268.
25. Vorgerd, M., van der Ven, P.F.M., Bruchertseifer, V., Löwe, T., Kley, R.A., Schröder, R., Lochmüller, H., Himmel, M., Koehler, K., Fürst, D.O., and Huebner, A. (2005). A mutation in the dimerization domain of filamin c causes a novel type of autosomal dominant myofibrillar myopathy. Am. J. Hum. Genet. *77*, 297–304.
26. Shatunov, A., Olivé, M., Odgerel, Z., Stadelmann-Nessler, C., Irlbacher, K., van Landeghem, F., Bayarsaikhan, M., Lee, H.S., Goudeau, B., Chinnery, P.F., et al. (2009). In-frame deletion in the seventh immunoglobulin-like repeat of filamin C in a family with myofibrillar myopathy. Eur. J. Hum. Genet. *17*, 656–663.
27. Nakamura, F., Osborn, T.M., Hartemink, C.A., Hartwig, J.H., and Stossel, T.P. (2007). Structural basis of filamin A functions. J. Cell Biol. *179*, 1011–1025.

28. Sawyer, G.M., Clark, A.R., Robertson, S.P., and Sutherland-Smith, A.J. (2009). Disease-associated substitutions in the filamin B actin binding domain confer enhanced actin binding affinity in the absence of major structural disturbance: Insights from the crystal structures of filamin B actin binding domains. J. Mol. Biol. *390*, 1030–1047.
29. Feng, Y., and Walsh, C.A. (2004). The many faces of filamin: A versatile molecular scaffold for cell motility and signalling. Nat. Cell Biol. *6*, 1034–1038.
30. Hock, R.S. (1999). Filamin. In Guidebook to the cytoskeletal and motor proteins, T. Kreis and R. Vale, eds. (Oxford: Oxford University Press), pp. 94–97.
31. Gorlin, J.B., Yamin, R., Egan, S., Stewart, M., Stossel, T.P., Kwiatkowski, D.J., and Hartwig, J.H. (1990). Human endothelial actin-binding protein (ABP-280, nonmuscle filamin): A molecular leaf spring. J. Cell Biol. *111*, 1089–1105.
32. Janmey, P.A. (1991). Mechanical properties of cytoskeletal polymers. Curr. Opin. Cell Biol. *3*, 4–11.
33. Weihing, R.R. (1988). Actin-binding and dimerization domains of HeLa cell filamin. Biochemistry *27*, 1865–1869.
34. Stossel, T.P., Condeelis, J., Cooley, L., Hartwig, J.H., Noegel, A., Schleicher, M., and Shapiro, S.S. (2001). Filamins as integrators of cell mechanics and signalling. Nat. Rev. Mol. Cell Biol. *2*, 138–145.
35. Linnemann, A., van der Ven, P.F.M., Vakeel, P., Albinus, B., Simonis, D., Bendas, G., Schenk, J.A., Micheel, B., Kley, R.A., and Fürst, D.O. (2010). The sarcomeric Z-disc component myopodin is a multiadapter protein that interacts with filamin and alpha-actinin. Eur. J. Cell Biol. *89*, 681–692.
36. Faulkner, G., Pallavicini, A., Comelli, A., Salamon, M., Bortoletto, G., Ievolella, C., Trevisan, S., Kojic', S., Dalla Vecchia, F., Laveder, P., et al. (2000). FATZ, a filamin-, actinin-, and telethonin-binding protein of the Z-disc of skeletal muscle. J. Biol. Chem. *275*, 41234–41242.
37. Thompson, T.G., Chan, Y.M., Hack, A.A., Brosius, M., Rajala, M., Lidov, H.G., McNally, E.M., Watkins, S., and Kunkel, L.M. (2000). Filamin 2 (FLN2): A muscle-specific sarcoglycan interacting protein. J. Cell Biol. *148*, 115–126.
38. Dalkilic, I., Schienda, J., Thompson, T.G., and Kunkel, L.M. (2006). Loss of FilaminC (FLNc) results in severe defects in myogenesis and myotube structure. Mol. Cell. Biol. *26*, 6522–6534.
39. Taveau, M., Bourg, N., Sillon, G., Roudaut, C., Bartoli, M., and Richard, I. (2003). Calpain 3 is activated through autolysis within the active site and lyses sarcomeric and sarcolemmal components. Mol. Cell. Biol. *23*, 9127–9135.
40. Luan, X., Hong, D., Zhang, W., Wang, Z., and Yuan, Y. (2010). A novel heterozygous deletion-insertion mutation (2695-2712 del/GTTTGT ins) in exon 18 of the filamin C gene causes filaminopathy in a large Chinese family. Neuromuscul. Disord. *20*, 390–396.
41. Selcen, D., Ohno, K., and Engel, A.G. (2004). Myofibrillar myopathy: Clinical, morphological and genetic studies in 63 patients. Brain *127*, 439–451.
42. Schröder, R., and Schoser, B. (2009). Myofibrillar myopathies: A clinical and myopathological guide. Brain Pathol. *19*, 483–492.
43. Clark, A.R., Sawyer, G.M., Robertson, S.P., and Sutherland-Smith, A.J. (2009). Skeletal dysplasias due to filamin A mutations result from a gain-of-function mechanism distinct from allelic neurological disorders. Hum. Mol. Genet. *18*, 4791–4800.
44. Gimona, M., Djinovic-Carugo, K., Kranewitter, W.J., and Winder, S.J. (2002). Functional plasticity of CH domains. FEBS Lett. *513*, 98–106.
45. Robertson, S.P., Twigg, S.R., Sutherland-Smith, A.J., Biancalana, V., Gorlin, R.J., Horn, D., Kenwrick, S.J., Kim, C.A., Morava, E., Newbury-Ecob, R., et al; OPD-spectrum Disorders Clinical Collaborative Group. (2003). Localized mutations in the gene encoding the cytoskeletal protein filamin A cause diverse malformations in humans. Nat. Genet. *33*, 487–491.
46. Bicknell, L.S., Morgan, T., Bonafé, L., Wessels, M.W., Bialer, M.G., Willems, P.J., Cohn, D.H., Krakow, D., and Robertson, S.P. (2005). Mutations in FLNB cause boomerang dysplasia. J. Med. Genet. *42*, e43.
47. Krakow, D., Robertson, S.P., King, L.M., Morgan, T., Sebald, E.T., Bertolotto, C., Wachsmann-Hogiu, S., Acuna, D., Shapiro, S.S., Takafuta, T., et al. (2004). Mutations in the gene encoding filamin B disrupt vertebral segmentation, joint formation and skeletogenesis. Nat. Genet. *36*, 405–410.
48. Roberts, R.G., Gardner, R.J., and Bobrow, M. (1994). Searching for the 1 in 2,400,000: A review of dystrophin gene point mutations. Hum. Mutat. *4*, 1–11.
49. Kaplan, J.M., Kim, S.H., North, K.N., Rennke, H., Correia, L.A., Tong, H.Q., Mathis, B.J., Rodríguez-Pérez, J.C., Allen, P.G., Beggs, A.H., and Pollak, M.R. (2000). Mutations in ACTN4, encoding alpha-actinin-4, cause familial focal segmental glomerulosclerosis. Nat. Genet. *24*, 251–256.
50. Kuhlman, P.A., Hemmings, L., and Critchley, D.R. (1992). The identification and characterisation of an actin-binding site in alpha-actinin by mutagenesis. FEBS Lett. *304*, 201–206.
51. Way, M., Pope, B., and Weeds, A.G. (1992). Evidence for functional homology in the F-actin binding domains of gelsolin and alpha-actinin: Implications for the requirements of severing and capping. J. Cell Biol. *119*, 835–842.
52. Galkin, V.E., Orlova, A., Salmazo, A., Djinovic-Carugo, K., and Egelman, E.H. (2010). Opening of tandem calponin homology domains regulates their affinity for F-actin. Nat. Struct. Mol. Biol. *17*, 614–616.
53. Ozanne, D.M., Brady, M.E., Cook, S., Gaughan, L., Neal, D.E., and Robson, C.N. (2000). Androgen receptor nuclear translocation is facilitated by the f-actin cross-linking protein filamin. Mol. Endocrinol. *14*, 1618–1626.
54. Loy, C.J., Sim, K.S., and Yong, E.L. (2003). Filamin-A fragment localizes to the nucleus to regulate androgen receptor and coactivator functions. Proc. Natl. Acad. Sci. USA *100*, 4562–4567.
55. Berry, F.B., O'Neill, M.A., Coca-Prados, M., and Walter, M.A. (2005). FOXC1 transcriptional regulatory activity is impaired by PBX1 in a filamin A-mediated manner. Mol. Cell. Biol. *25*, 1415–1424.
56. Uribe, R., and Jay, D. (2009). A review of actin binding proteins: New perspectives. Mol. Biol. Rep. *36*, 121–125.
57. Goetsch, S.C., Martin, C.M., Embree, L.J., and Garry, D.J. (2005). Myogenic progenitor cells express filamin C in developing and regenerating skeletal muscle. Stem Cells Dev. *14*, 181–187.
58. Cirak, S., von Deimling, F., Sachdev, S., Errington, W.J., Herrmann, R., Bönnemann, C., Brockmann, K., Hinderlich, S., Lindner, T.H., Steinbrecher, A., et al. (2010). Kelch-like homologue 9 mutation is associated with an early onset autosomal dominant distal myopathy. Brain *133*, 2123–2135.